Photochemistry of the organoselenium compound ebselen: direct photolysis and reaction with active intermediates of conventional reactive species sensitizers and quenchers

Journal:	*Environmental Science & Technology*
Manuscript ID	es-2020-03093w.R2
Manuscript Type:	Article
Date Submitted by the Author:	n/a
Complete List of Authors:	Hopanna, Mamatha; University of Maryland Baltimore County, Chemical, Biochemical and Environmental Engineering Kelly, Lisa; University of Maryland Baltimore County, Chemistry and Biochemistry Blaney, Lee; University of Maryland Baltimore County, Chemical, Biochemical and Environmental Engineering

Photochemistry of the organoselenium compound ebselen: direct photolysis and reaction with active intermediates of conventional reactive species sensitizers and quenchers

Mamatha Hopanna [1], Lisa Kelly [2], and Lee Blaney [1*]

1: University of Maryland Baltimore County
Department of Chemical, Biochemical, and Environmental Engineering
1000 Hilltop Circle, Engineering Building 314
Baltimore, MD 21250 USA

2: University of Maryland Baltimore County
Department of Chemistry and Biochemistry
1000 Hilltop Circle
Baltimore, MD 21250 USA

* Corresponding author:
Lee Blaney, PhD
University of Maryland Baltimore County
Department of Chemical, Biochemical, and Environmental Engineering
1000 Hilltop Circle, ECS 314
Baltimore, MD 21250 USA
Tel: +1-410-455-8608
Fax: +1-410-455-1049
Email: blaney@umbc.edu

ABSTRACT

Ebselen (EBS), 2-phenyl-1,2-benzisoselenazol-3(2H)-one, is an organoselenium pharmaceutical with antioxidant and anti-inflammatory properties. Furthermore, EBS is an excellent scavenger of reactive oxygen species. This property complicates conventional protocols for sensitizing and quenching reactive species due to potential generation of active intermediates that quickly react with EBS. In this study, the photochemical reactivity of EBS was investigated in the presence of (1) $^1O_2$ and $^\bullet OH$ sensitizers (Rose Bengal (RB), perinaphthanone, H_2O_2) and (2) reactive species scavenging and quenching agents (sorbic acid, isopropanol, sodium azide, *tert*-butanol) that are commonly employed to study photodegradation mechanisms and kinetics. The carbon analog of EBS, namely 2-phenyl-3H-isoindol-1-one, was included as a reference compound to confirm the impact of the selenium atom on EBS photochemical reactivity. EBS does not undergo acid dissociation, but pH-dependent kinetics were observed in RB-sensitized solutions, suggesting EBS reaction with active intermediates ($^3RB^{2-*}$, $O_2^{\bullet-}$, H_2O_2) that are not kinetically-relevant for other compounds. In addition, the observed rate constant of EBS increased in the presence of sorbic acid, isopropanol, and sodium azide. These findings suggest that conventional reactive species sensitizers, scavengers, and quenchers need to be carefully applied to highly reactive organoselenium compounds to account for reactions that are typically slow for other organic contaminants.

Keywords: ebselen; reactive oxygen species; active intermediate; organometallic; photochemistry; selenium

47 **GRAPHICAL ABSTRACT**

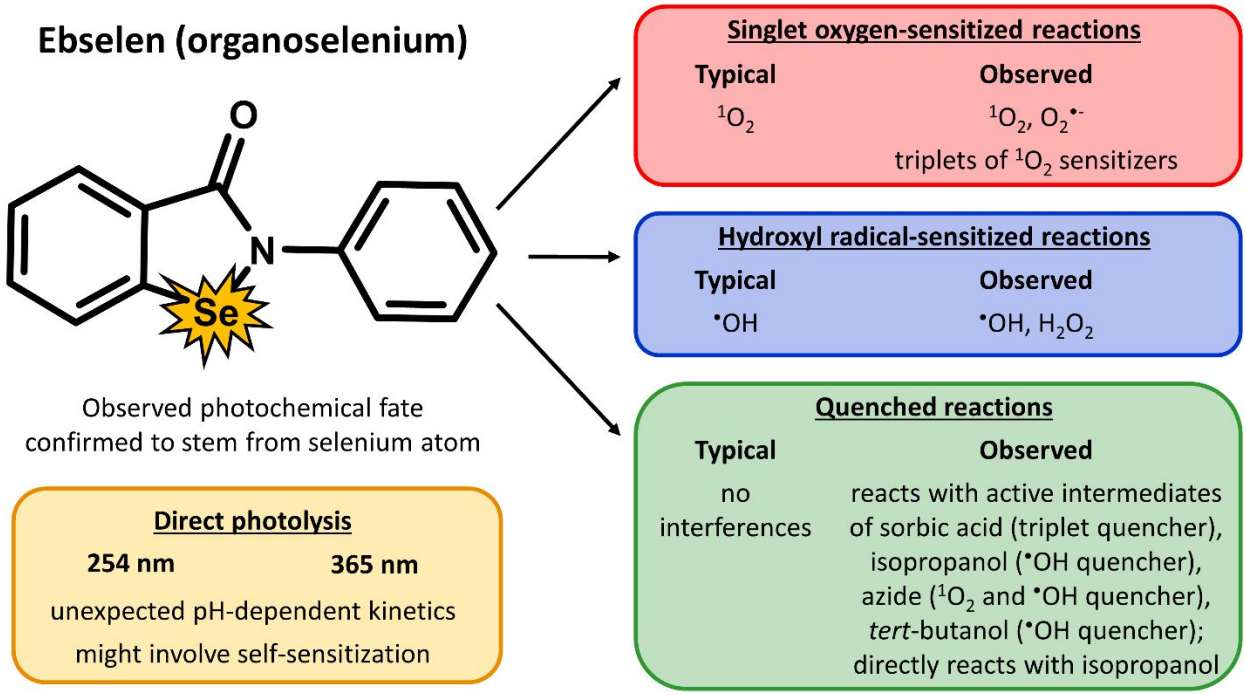

48

1. INTRODUCTION

Ebselen (EBS) is an organoselenium compound with anti-inflammatory, anti-atherosclerotic, and cytoprotective properties [1, 2]. Currently, EBS is mostly used as an antioxidant and glutathione peroxidase mimic [3, 4]. Ongoing clinical trials are investigating EBS as a treatment for reperfusion injury, stroke, hearing loss, and bipolar disorder [5]. EBS has also emerged as a promising treatment for clinical isolates of multidrug-resistant *Staphylococcus aureus* [6, 7]. Most recently, Jin *et al.* reported that out of more than 10,000 compounds investigated by structure-based and high-throughput screening, EBS emerged as the only compound with promising antiviral activity against COVID-19 in cell-based assays [8]. A recent PubMed database search found more than 1000 publications on EBS, with many focused on potential therapeutic applications or synthesis of EBS analogs or derivatives. For these reasons, organoselenium compounds represent a new class of contaminants of emerging concern.

The aforementioned pharmaceutical applications stem from the biochemical properties of EBS, including its excellent scavenging of reactive oxygen species, such as singlet oxygen ($^1O_2$), hydrogen peroxide (H_2O_2), and peroxynitrite ($OONO^-$) [2, 9, 10]. However, EBS can also cause cellular toxicity. For example, EBS induced necrotic cell death, DNA damage, genotoxicity, and apoptosis at high concentrations [11-13]. Several studies have also reported acute and chronic effects of selenium on fish and wildlife at concentrations of 1-5 μg L^{-1} [14, 15]. Based on recent scientific findings, EPA set a new national chronic aquatic life criterion for selenium in 2016 [16]. Although metabolic studies suggest that selenium is not immediately released from EBS, the fate of EBS in abiotic environmental systems and water/wastewater treatment processes is unknown. Due to its

antioxidant properties, EBS is expected to exhibit fast photodegradation kinetics in natural water bodies, where reactive oxygen species are generated through indirect photolysis. However, the photochemical reactivity and degradation mechanisms of EBS are unknown and warrant investigation.

Previous studies have identified the kinetic relevance of both direct and indirect photolysis mechanisms to photodegradation of organic contaminants in engineered and natural systems [17, 18]. The rate constants for photodegradation mechanisms are typically determined in well-controlled laboratory experiments and then applied to calculate the half-lives of contaminants in the natural environment [19-21]. The corresponding experimental protocols employ reactive species sensitizers, such as Rose Bengal (RB; for $^1O_2$), perinaphthanone (PN; for $^1O_2$ and surrogate for triplet dissolved organic matter ($^3DOM^*$)), and Suwannee River Natural Organic Matter (for $^1O_2$, hydroxyl radicals ($^\bullet OH$), and $^3DOM^*$). In addition, reactive species scavengers and quenchers, such as sorbic acid (for triplets, also prevents $^1O_2$ production), sodium azide (NaN_3; for $^1O_2$ and $^\bullet OH$), isopropanol (for $^\bullet OH$), and *tert*-butanol (for $^\bullet OH$), are used to inhibit certain reaction mechanisms and isolate others. Together, these tools facilitate determination of specific rate constants for organic contaminants with individual reactive species.

We hypothesize that the antioxidant properties of EBS [2, 9, 10] will pose challenges to the use of conventional protocols for sensitizing and quenching reactive species due to generation of active intermediates that quickly react with EBS. For example, RB forms the following transient species: triplet RB ($^3RB^{2-*}$); $RB^{\bullet 3-}$; $RB^{\bullet -}$; $^1O_2$; and, superoxide anion radical ($O_2^{\bullet -}$) [22, 23]. As indicated in Figure 1, $^3RB^{2-*}$, $RB^{\bullet 3-}$, and $RB^{\bullet -}$ are not kinetically relevant for many organic

chemicals; therefore, many studies do not consider these reactions [24, 25]. If reactions between RB active intermediates and the organic chemical are kinetically relevant but not considered, the calculated second-order rate constant for $^1O_2$ reaction with that chemical would be over-estimated by RB-sensitized experiments. Criado *et al.* [22] observed fast reactions between tryptophan and $^3RB^{2-*}$ with rate constants on the order of 10^7 M^{-1} s^{-1}. In solution, $^3RB^{2-*}$ is quenched by molecular oxygen in a reaction that yields 75% $^1O_2$ and 20% $O_2^{\bullet-}$ [24]. While most studies focus on the $^1O_2$ product, select tryptophan derivatives can also react with $O_2^{\bullet-}$ at kinetically-relevant rates [22]. Similarly, Davis *et al.* [26] reported the high reactivity of fenamates with triplet PN, which stems from the use of PN as a $^1O_2$ and triplet sensitizer.

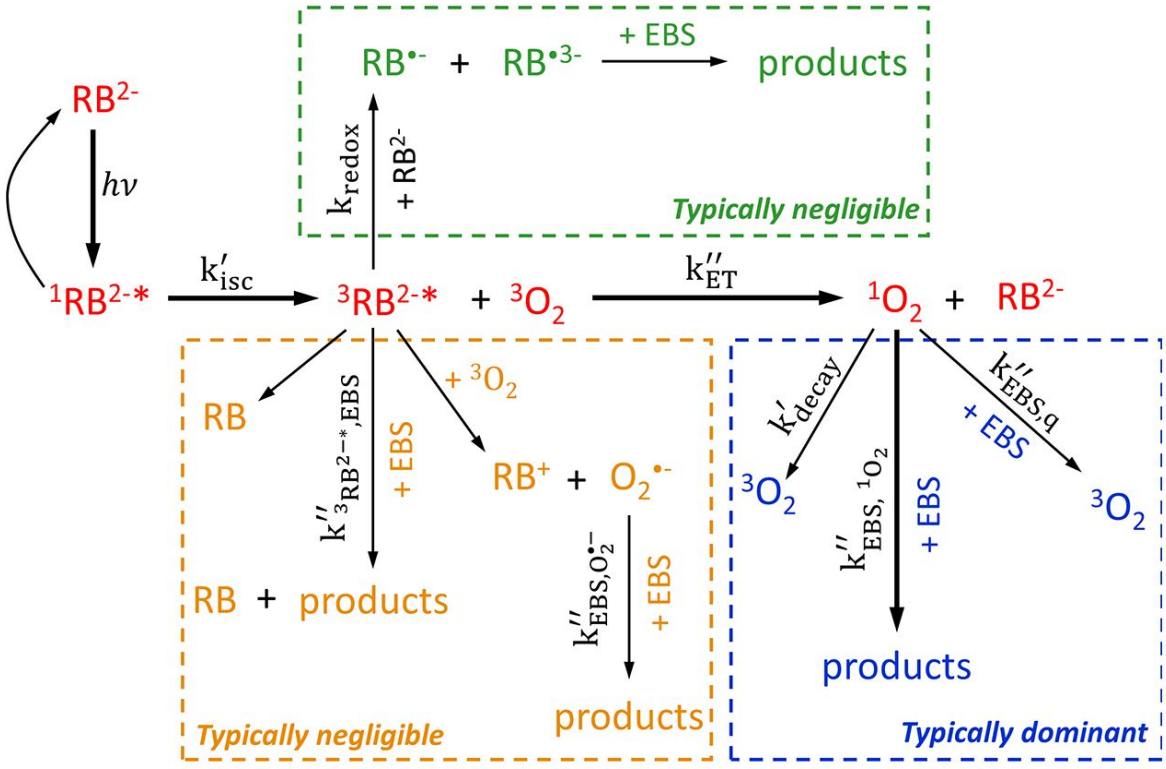

Figure 1. Photochemistry of RB and proposed reactions with EBS. The rate constants indicated in the figure are defined as follows: $\mathbf{k'_{isc}}$, rate constant for inter-system crossing of $^1RB^{2-*}$ to $^3RB^{2-*}$; $\mathbf{k''_{ET}}$, rate constant for energy transfer reaction from $^3RB^{2-*}$ to molecular oxygen, $^3O_2$; $\mathbf{k''_{^3RB^{2-*},EBS}}$, rate constant for

energy transfer reaction from $^3RB^{2-*}$ to EBS; $\mathbf{k''_{EBS,O_2^{\bullet-}}}$, second-order rate constant for EBS reduction by $\mathbf{O_2^{\bullet-}}$; $\mathbf{k'_{decay}}$, rate constant for $^1O_2$ decay to $^3O_2$; $\mathbf{k''_{EBS,^1O_2}}$, second-order rate constant for EBS reaction with $^1O_2$ (chemical quenching); $\mathbf{k''_{EBS,q}}$, second-order rate constant for physical quenching of $^1O_2$ by EBS; and, $\mathbf{k_{redox}}$, rate constant for reduction of $^3RB^{2-*}$ by RB^{2-}. The thick, black reaction arrows emphasize the reactions typically considered in RB-sensitized experiments. The RB photochemistry was adapted from previous literature [22, 23] to elucidate potential reaction pathways for EBS.

Other chemicals used to sensitize, scavenge, or quench reactive species also produce triplets and/or active intermediate radicals (see Table S1 in the Supporting Information (SI)) [5, 27, 28]. As noted above, EBS is an excellent scavenger of reactive species; therefore, secondary reactions must be carefully examined to ensure proper calculation of second-order rate constants for specific reactions. For example, secondary organic radicals (*e.g.*, R• and ROO•), which are often kinetically negligible, are formed by the reaction of *tert*-butanol with •OH [5]. If EBS reacts with the R• or ROO• active intermediates, the use of *tert*-butanol to quench •OH can lead to other unaccounted mechanisms. Packer *et al.* [29] reported similar observations when using isopropanol to quench radicals during photodegradation of clofibric acid and diclofenac. Addition of 1% isopropanol (v/v) increased the photodegradation rates for clofibric acid and diclofenac by 1.7× and 1.45×, respectively, compared to those observed in deionized (DI) water. One reason for the enhanced phototransformation kinetics was formation of active isopropanol intermediates. Unless carefully examined, these reactions can lead to calculation of inaccurate rate constants.

The heightened interest in organoselenium pharmaceuticals coupled to the general lack of knowledge regarding the photochemistry of these molecules motivated the present study. We

hypothesized that the selenium atom in EBS would participate in complex photochemical reactions that are difficult to capture using conventional sensitization and quenching protocols. The overall goal of this study was to investigate the photochemical reactivity of EBS with (1) $^1O_2$ and $^{\bullet}OH$ sensitizers (*i.e.*, RB, PN, and H_2O_2) and (2) reactive species scavenging and quenching agents (*i.e.*, isopropanol, sodium azide, sorbic acid, and *tert*-butanol) that are commonly employed to study the fate of organic contaminants during direct and indirect photolysis. To determine the role of the selenium atom in direct and indirect photochemical reactions, we examined the fate of the EBS carbon analog (*i.e.*, 2-phenyl-3H-isoindol-1-one (C-EBS), namely EBS but with a carbon atom substituted for the selenium atom). To establish the baseline photoreactivity, wavelength-dependent, pseudo-first-order rate constants and quantum yields were evaluated for direct photolysis of EBS and C-EBS. Although this work specifically focused on EBS, the outcomes contribute to overall understanding of organoselenium photochemistry.

2. MATERIALS AND METHODS

2.1. Chemicals

Details on the chemical reagents used in experiments are included in Text S1 of the SI.

2.2. Analytical methods

The analytical methods employed for quantitation of EBS, C-EBS, *para*-chlorobenzoic acid (*p*CBA; •OH probe), and furfuryl alcohol (FFA; $^1O_2$ probe) are described in Text S2 of the SI.

2.3. Photolysis experiments

All photochemical experiments were performed in an eight-position, merry-go-round Rayonet reactor (Southern New England Ultraviolet Inc.; Branford, CT) equipped with eight bulbs emitting (i) monochromatic light at 254 nm or (ii) across the 310-410 nm range with a peak at 365 nm (labeled 365 nm, below). The 254-nm and 365-nm bulbs were used to sensitize the production of •OH and $^1O_2$, respectively. Moreover, the 254-nm and 365-nm light sources were representative of UV disinfection processes in drinking water and wastewater treatment plants and the high-energy solar irradiation that reaches surface water, respectively, providing insight to direct photolysis of EBS in these systems. The average incident photon flux for the 254-nm and 365-nm systems were calculated to be 2.71 (± 0.18) × 10^{-5} Ein L^{-1} s^{-1} and 1.93 (± 0.40) × 10^{-5} Ein L^{-1} s^{-1}, respectively, using the ferrioxalate actinometer [30, 31]; note, error values refer to the standard deviation of three measurements. To determine the direct photolysis kinetics, experimental solutions contained 3.6 μM EBS or C-EBS and 5 mM phosphate buffer in DI water. Experimental solutions were irradiated in quartz tubes with an inner diameter of 1.5 cm. Samples were collected at predetermined times and stored at -20 °C in amber vials prior to analysis by liquid chromatography with triple quadrupole tandem mass spectrometry (LC-MS/MS) or high-performance liquid chromatography with UV absorbance detection. Dark controls were included to account for other reactions, including hydrolysis and direct reaction of

177 EBS with reactive species quenchers, scavengers, and sensitizers. All experiments were
178 conducted at room temperature (*i.e.*, 22 ± 1°C).
179
180 ***2.3.1. Reactivity of EBS with $^1O_2$ sensitizers***
181
182 The photoreactivity of EBS in solutions containing the RB and PN $^1O_2$ sensitizers was
183 investigated at 365 nm. Experimental solutions contained 3.6 μM EBS, 5 μM RB or 0.5 μM PN,
184 0.2 mM FFA, and 5 mM phosphate buffer in DI water. Test conditions included five pH values
185 between 4.4 and 10.2. The experiments were conducted at similar conditions with C-EBS to
186 determine the importance of the selenium atom on EBS reactivity with $^1O_2$; however, the RB
187 concentration was increased to 40 μM for the C-EBS experiments due to the slower reaction
188 between C-EBS and $^1O_2$ observed in preliminary investigations. The steady-state $^1O_2$
189 concentration (*i.e.*, $[^1O_2]_{ss}$) was calculated by dividing the observed pseudo-first-order rate
190 constant for FFA degradation by its second-order rate constant with $^1O_2$ (*i.e.*, $k''_{^1O_2,\,FFA} = 1.0 \times 10^8$
191 $M^{-1}\,s^{-1}$ [32]). In separate experiments, 5 and 10 mM NaN_3 were added to the experimental solutions
192 to quench $^1O_2$ (as it was produced) and investigate EBS degradation by triplets or active
193 intermediates of the RB and PN sensitizers.
194
195 ***2.3.2. Reactivity of EBS with $^{\bullet}OH$ sensitizers***
196
197 Conventional methods of generating $^{\bullet}OH$, such as UV-H_2O_2, photo-Fenton reactions, and solar
198 irradiation of NO_3^- or NO_2^- [33], may complicate evaluation of EBS degradation kinetics due to
199 secondary reactions with H_2O_2, $ONOO^-$, or other active intermediates [10, 34, 35]. For this reason,

sodium pyruvate was employed as a non-radical-forming H_2O_2 quenching agent. The suitability of pyruvate was investigated in the dark using the following solutions: (i) 0.36-36 μM EBS; (ii) 0.36-36 μM EBS + 7.5 mM sodium pyruvate; (iii) 0.36-36 μM EBS + 0.5 mM H_2O_2; and, (iv) 0.36-36 μM EBS + 0.5 mM H_2O_2 + 7.5 mM sodium pyruvate. These solutions were always generated by first adding EBS, then sodium pyruvate (when applicable), and then H_2O_2 (when applicable). To confirm the extent of H_2O_2 quenching by pyruvate, EBS concentrations in these samples were analyzed immediately after preparation and again after 24 h of storage in the dark.

The second-order rate constant for EBS reaction with H_2O_2 was determined in the dark. The 10-mL experimental solutions contained 3.6 μM EBS, 50 μM H_2O_2, and 5 mM phosphate buffer (pH 7.0 ± 0.1). An excess of H_2O_2 was added to allow calculation of the pseudo-first-order rate constant [19]; in particular, the initial concentration ratio of H_2O_2 to EBS was 15 mol/mol to ensure that residual EBS concentrations were above the analytical limits of quantitation. Samples (100 μL) were collected at designated times and deposited into vials containing 900 μL of 7.5 mM sodium pyruvate to immediately quench the H_2O_2 residual. The second-order rate constant for EBS reaction with H_2O_2 (k''_{EBS,H_2O_2}) was calculated by dividing the observed pseudo-first-order rate constant of EBS ($k'_{EBS,obs}$) by the molar H_2O_2 concentration ($[H_2O_2]$), as indicated in Eq. 1.

$$k''_{EBS,H_2O_2} = \frac{k'_{EBS,obs}}{[H_2O_2]} \quad \text{(Eq. 1)}$$

The second-order rate constant for EBS reaction with •OH ($k''_{EBS,•OH}$) was measured by competition kinetics with *p*CBA. Experimental solutions containing 3.6 μM EBS, 5 μM H_2O_2, 75

μM *p*CBA, and 5 mM phosphate buffer (pH 7.0 ± 0.1) were irradiated at 254 nm. Samples (100 μL) collected at designated times were mixed with 900 μL of 7.5 mM sodium pyruvate to quench the H_2O_2 residual and inhibit further reactions. EBS could have degraded by direct photolysis, reaction with H_2O_2, or reaction with •OH. The *p*CBA probe molecule can undergo similar reactions, but the H_2O_2 reaction is not kinetically relevant [36]. The integrated mass balance expressions for EBS and *p*CBA in the batch reactors are shown in Eq. 2 and Eq. 3, respectively.

$$-\ln\frac{[\mathrm{EBS}]_t}{[\mathrm{EBS}]_0} = k'_{d,\mathrm{EBS}}t + k''_{\mathrm{EBS},H_2O_2}[H_2O_2]t + k''_{\mathrm{EBS},^{\bullet}OH}\int_0^t [^{\bullet}OH]\,dt \quad \text{(Eq. 2)}$$

$$-\ln\frac{[p\mathrm{CBA}]_t}{[p\mathrm{CBA}]_0} = k'_{d,p\mathrm{CBA}}t + k''_{p\mathrm{CBA},^{\bullet}OH}\int_0^t [^{\bullet}OH]\,dt \quad \text{(Eq. 3)}$$

The variables in Eq. 2 and 3 are defined as follows: t is the irradiation time (s); $[\mathrm{EBS}]_0$ and $[\mathrm{EBS}]_t$ are the EBS concentrations (μM) at time 0 and t, respectively; $[p\mathrm{CBA}]_0$ and $[p\mathrm{CBA}]_t$ are the *p*CBA concentrations (μM) at time 0 and t, respectively; $k'_{d,\mathrm{EBS}}$ and $k'_{d,p\mathrm{CBA}}$ are apparent time-based pseudo-first-order rate constants for direct photolysis of EBS and *p*CBA at 254 nm, respectively; and, $k''_{p\mathrm{CBA},^{\bullet}OH}$ is the second-order rate constant for *p*CBA reaction with •OH (*i.e.*, 5.2×10^9 $M^{-1}s^{-1}$ [37]).

As EBS and *p*CBA were present in the same reactor, the hydroxyl radical exposure (*i.e.,* $\int_0^t [^\bullet OH]\, dt$) in Eq. 2 is equal to that in Eq. 3. These expressions can, therefore, be rearranged as shown in Eq. 4, which was used to solve for $k''_{EBS,^\bullet OH}$ [18].

$$\left[\ln\left(\frac{[EBS]}{[EBS]_0}\right) + k'_{d,EBS}t + k''_{EBS,H_2O_2}[H_2O_2]t\right] = \left[\ln\left(\frac{[pCBA]}{[pCBA]_0}\right) + k'_{d,pCBA}t\right]\frac{k''_{EBS,^\bullet OH}}{k''_{pCBA,^\bullet OH}} \quad \text{(Eq. 4)}$$

A similar experimental design was employed to calculate second-order rate constants for C-EBS with $^\bullet OH$; however, the H_2O_2 concentration was increased to 5 mM due to the lower observed reactivity of C-EBS with $^\bullet OH$ (compared to EBS).

2.3.3 Reactivity of EBS with scavengers and quenchers

The reactivity of EBS with reactive species scavenging and quenching molecules, and associated triplets or active intermediates, was investigated by irradiating 3.6 μM EBS in the presence of 0.5 mM sorbic acid (triplet quencher, also prevents $^1O_2$ production) or 50-100 mM isopropanol ($^\bullet OH$ quencher) at 365 nm. All solutions were buffered at pH 7.0 ± 0.1 with 5 mM phosphate buffer. Furthermore, the reactivity of EBS in the presence of 0, 1, and 10 mM NaN_3 ($^1O_2$ and $^\bullet OH$ quencher) was investigated at 254 nm and 365 nm, with solution pH adjusted to 4, 6, 8, and 10 by 5 mM phosphate buffer.

Secondary organic radicals (*e.g.*, R• and ROO•) formed through *tert*-butanol reaction with •OH [5] might react with EBS. To examine whether these reactions were kinetically relevant, experimental solutions containing 3.6 μM EBS, 5 μM H_2O_2, 10-100 mM *tert*-butanol, and 5 mM phosphate buffer (pH 7.0 ± 0.2) were irradiated at 254 nm. Samples (100 μL) from the above experiments were collected at designated times and deposited into vials containing 900 μL of 7.5 mM sodium pyruvate to quench further reactions.

3. RESULTS AND DISCUSSION

3.1 Direct photolysis of EBS and C-EBS

The apparent molar absorption coefficient and quantum yield dictate the extent of chemical degradation by direct photolysis. The molar absorption coefficients of EBS and C-EBS are shown for 230-380 nm and pH 4.5, 7.0, and 9.5 in Figure S1 of the SI. Due to their aromatic moieties, EBS and C-EBS both absorb UVC light, and the apparent molar absorption coefficients at 254 nm were 1.22 (± 0.01) × 10^4 M^{-1} cm^{-1} and 6.91 (± 0.11) × 10^3 M^{-1} cm^{-1}, respectively; note, the error corresponds to standard deviation (n = 3). Compared to C-EBS, EBS exhibited extended absorbance into the UVA region (up to 370 nm), presumably due to the presence of the selenium atom, which was the only difference between the two chemicals. Neither compound undergoes acid dissociation, and both compounds are present in solution as neutral molecules. For these reasons, solution pH had a negligible influence on the absorbance spectra (see Figure S1 in the SI).

287

288 The degradation kinetics of EBS and C-EBS were investigated at pH 7 for direct photolysis at
289 254 nm and 365 nm. The observed pseudo-first-order rate constants at 254 nm for EBS and C-
290 EBS were 2.74 (± 0.20) × 10^{-3} s^{-1} and 8.50 (± 0.32) × 10^{-4} s^{-1}, respectively. Phototransformation
291 reactions were slower for irradiation with light at 365 nm, wherein the observed rate constant for
292 EBS transformation was 5.17 (± 0.95) × 10^{-5} s^{-1} and C-EBS showed negligible degradation
293 kinetics ($k'_{d,C-EBS} < 2.3 \times 10^{-6}$ s^{-1}). The error values reported above correspond to 95%
294 confidence intervals on the mean rate constant calculated from time-series experiments (n = 14).
295 Using these rate constants, the apparent quantum yield was calculated (see Text S3 and Eq. S1 in
296 the SI). The apparent quantum yields at 254 nm for EBS and C-EBS were 13.6 (± 0.1) × 10^{-2} mol
297 Ein^{-1} and 2.0 (± 0.7) × 10^{-2} mol Ein^{-1}, respectively. For 365 nm, EBS exhibited an apparent
298 quantum yield of 1.4 (± 0.1) × 10^{-3} mol Ein^{-1}; however, the quantum yield of C-EBS at 365 nm
299 was much lower ($\phi_{C\text{-}EBS,365} < 2.8 \times 10^{-5}$ mol Ein^{-1}). Due to the low extent of degradation, the
300 reported quantum yield for C-EBS at 365 nm was an upper-bound estimate included to
301 contextualize the differences between EBS and C-EBS reactivity.

302

303 The observed pseudo-first-order rate constants for EBS photodegradation are summarized in
304 Table 1. At 254 nm, EBS exhibited pH-dependent photodegradation with the observed rate
305 constant increasing from 1.73 (± 0.27) × 10^{-3} s^{-1} at pH 4.4 to 13.50 (± 0.43) × 10^{-3} s^{-1} at pH 10.5.
306 Solution pH exerted a similar effect on EBS photodegradation at 365 nm, but the magnitude of
307 the change in observed rate constant was much lower. The pseudo-first-order rate constants at
308 254 nm and 365 nm increased by 680% and 73%, respectively, across the pH 4.4-10.5 range.
309 The faster EBS photoreaction kinetics observed at higher pH were not expected because (i) EBS

does not dissociate and (ii) the measured molar absorption coefficients were similar for the pH 4.5-9.5 range. A potentiometric titration was conducted and confirmed the absence of environmentally-relevant acid dissociation sites; furthermore, the ChemAxon structure-based algorithm [38] did not identify an acid dissociation site in the pH 0-14 range. Previous studies indicated that phosphate buffer can promote photoreduction and/or photoaddition mechanisms [39, 40]; however, Figure S2 in the SI highlights insignificant impacts on EBS degradation for solutions containing 0, 10, 20, and 30 mM phosphate buffer at pH 7.2.

Table 1. Observed pseudo-first-order rate constants for direct photolysis of EBS with light at 254 nm and 365 nm.

Solution pH	Observed rate constant (s^{-1})	
	254 nm	**365 nm**
4.4	1.73 (± 0.27) × 10^{-3}	3.45 (± 0.36) × 10^{-5}
5.1	1.80 (± 0.58) × 10^{-3}	3.14 (± 0.48) × 10^{-5}
6.3	2.59 (± 0.21) × 10^{-3}	4.77 (± 0.66) × 10^{-5}
6.9	2.74 (± 0.20) × 10^{-3}	5.17 (± 0.95) × 10^{-5}
7.8	4.18 (± 0.10) × 10^{-3}	5.41 (± 0.87) × 10^{-5}
8.3	7.22 (± 0.22) × 10^{-3}	5.60 (± 0.48) × 10^{-5}
9.4	8.88 (± 0.24) × 10^{-3}	5.34 (± 0.64) × 10^{-5}
10.5	13.50 (± 0.43) × 10^{-3}	5.98 (± 0.81) × 10^{-5}

The observed differences in direct photolysis kinetics may also stem from pH-dependent self-sensitized reactions. Photosensitized generation of reactive oxygen species by EBS may involve both type I (electron transfer reactions to produce $O_2^{\bullet-}$) and type II (energy transfer to molecular oxygen to produce $^1O_2$) reactions [24, 41], as shown in Eq. 5-8.

$$EBS + h\nu \rightarrow {}^1EBS^* \rightarrow {}^3EBS^* \quad \text{(Eq. 5)}$$

$$^3EBS^* + O_2 \rightarrow {}^1O_2 + EBS \quad \text{(Eq. 6)}$$

$$EBS + h\nu \rightarrow EBS^{\bullet+} + e_{aq}^- \quad \text{(Eq. 7)}$$

$$e_{aq}^- + O_2 \rightarrow O_2^{\bullet-} \quad \text{(Eq. 8)}$$

In Eq. 5-8, $^1EBS^*$ is excited singlet state EBS, $^3EBS^*$ is excited triplet state EBS, $EBS^{\bullet+}$ is EBS radical cation, and e_{aq}^- is a solvated electron.

To investigate the aforementioned mechanisms, transient absorption spectroscopy was conducted at 355 nm. Details of the instrument and data analysis are available in previous reports [42, 43] and Text S4 of the SI. Figure S3 in the SI demonstrates the absence of spectroscopic evidence for

345 $^3EBS^*$ and $EBS^{\bullet+}$ production at pH 4.4-11.2. These results suggest (i) low quantum yields of EBS
346 transients at the 355 nm excitation wavelength and/or (ii) low molar absorption coefficients of
347 transient species. The transient absorption spectroscopy results support the lower pH-dependence
348 of EBS rate constants at 365 nm reported in Table 1. However, the higher photoreactivity of EBS
349 at 254 nm, which stemmed from a 31× higher molar absorption coefficient and a 96× higher
350 quantum yield (compared to 365 nm), suggested that self-sensitized reactions may be more
351 evident for irradiation at 254 nm. While a detailed evaluation of the reaction mechanisms
352 involved with direct photolysis was outside of the scope of this study, the importance of
353 evaluating self-sensitized reactions and the influence of solution pH was identified for
354 organoselenium chemicals.
355
356 **3.2. EBS interactions with reactive species sensitizers**
357
358 ***3.2.1. Active intermediates of $^1O_2$ sensitizers react with EBS***
359
360 To sensitize the generation of $^1O_2$, solutions containing EBS were spiked with RB or PN and
361 irradiated at 365 nm. The observed pseudo-first-order rate constants for EBS degradation in the
362 RB-sensitized solutions are shown in Figure 2a. The observed rate constant increased from 7.03
363 (± 1.20) × 10^{-4} s^{-1} at pH 4.4 to 6.74 (± 1.80) × 10^{-3} s^{-1} at pH 10.2, corresponding to a 859%
364 increase; however, the steady-state $^1O_2$ concentrations were comparable, 3.1 (± 0.5) × 10^{-12} M,
365 for all pH conditions. The drastic change in observed rate constant coupled to the consistent $^1O_2$
366 concentration suggests the importance of other reaction mechanisms. While the rate constants for
367 direct photolysis at 365 nm also increased at higher solution pH, the magnitude (*i.e.*, 3-6 × 10^{-5} s^{-}

368 ^{1}) was about 100× lower than the observed rate constants for RB-sensitized experiments. Given
369 the absence of acid dissociation reactions and the relatively minor contribution of direct
370 photolysis at 365 nm, the faster photodegradation kinetics observed at higher pH in Figure 2a
371 were attributed to EBS reaction with triplets or active intermediates of RB (see Figure 1).
372 Similar results were observed in solutions containing PN (Figure S4 in the SI). Unlike EBS, C-
373 EBS exhibited low reactivity in RB-sensitized solutions, and the measured degradation was
374 negligible under all pH conditions (Figure S5 in the SI). These results suggest that the selenium
375 atom played a crucial role in the faster reaction kinetics observed at higher pH.
376

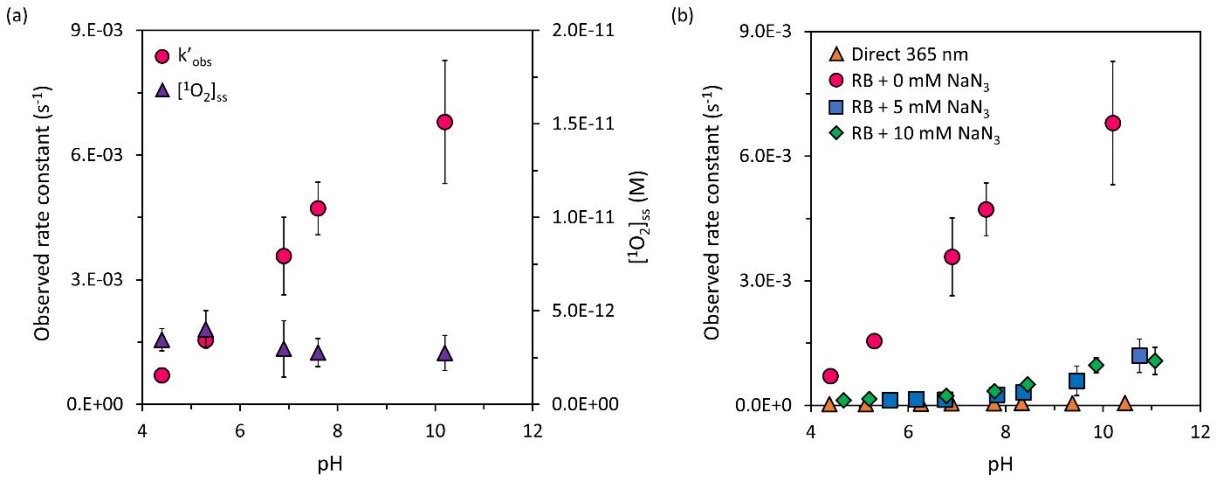

377

378 **Figure 2. Observed pseudo-first-order rate constants for EBS photodegradation at 365 nm in (a)**
379 **solutions that initially contained 3.6 µM EBS, 5 µM RB, and 0.2 mM FFA and (b) 5 µM RB-**
380 **sensitized solutions with 3.6 µM EBS and 0, 5, and 10 mM NaN_3 (no FFA).** Solution pH was
381 maintained with 5 mM phosphate buffer. The secondary y-axis in (a) shows steady-state $^1O_2$
382 concentrations. The symbols correspond to rate constants calculated from time series experiments (n = 7).
383 Error bars represent 95% confidence intervals on the mean rate constant from the time series experiments.
384
385

386 To confirm whether $^3RB^{2-*}$ or active intermediates contributed to EBS photodegradation, 5 and
387 10 mM NaN_3 were added to experimental solutions to quench $^1O_2$ produced by the RB system.
388 Even though NaN_3 quenches both $^1O_2$ and $^\bullet OH$, the quenching reaction is associated with $^1O_2$ as
389 the expected $^\bullet OH$ yield is low due to (1) the multistep reactions involved in $^\bullet OH$ generation
390 (electron transfer from $^3RB^{2-*}$ to $^3O_2$ to form $O_2^{\bullet-}$ → self-dismutation of $O_2^{\bullet-}$ → H_2O_2 irradiation
391 (254 nm)→ $^\bullet OH$), (2) the low initial concentration of RB (5 μM), and (3) the wavelength
392 employed in these experiments (365 nm). Based on the EBS and NaN_3 concentrations, the rate
393 constant for $^1O_2$ quenching by NaN_3 ($1.5 \times 10^9\ M^{-1}\ s^{-1}$ [44, 45]), and the rate constant for $^1O_2$ reaction
394 with EBS ($4.16 \times 10^6\ M^{-1}\ s^{-1}$ [9]), NaN_3 quenched more than 99.99% of $^1O_2$. Direct EBS reaction
395 with NaN_3 was kinetically negligible. Figure 2b indicates that the addition of NaN_3 suppressed
396 EBS photodegradation kinetics at all pH conditions, although the observed rate constants for
397 EBS degradation still increased from pH 7 to pH 11. No significant differences were identified
398 between the observed rate constants for the 5 and 10 mM NaN_3 conditions at any pH ($p > 0.10$,
399 ANCOVA), suggesting that these concentrations were sufficient to quench $^1O_2$ formed by the RB
400 sensitizer. With 10 mM NaN_3, the observed rate constant for EBS photodegradation was
401 suppressed (compared to the 0 mM NaN_3 condition) by 82% at pH 4.4, 90% at pH 7.0, and 86%
402 at pH 10.2; however, the observed rate constant for EBS degradation was enhanced (compared to
403 direct photolysis) by 72% at pH 4.4, 85% at pH 7.0, and 94% at pH 10.2. These results support
404 the kinetic relevance of other active intermediates produced by irradiation of RB (see Figure 1)
405 and/or NaN_3 (see section 3.3 for more details).
406
407 To further investigate the potential contributions of $^3RB^{2-*}$ to EBS degradation, transient
408 absorption studies were conducted under anoxic conditions, at varying solution pH, and with

409 incremental addition of EBS (see Text S4 of the SI). An excitation wavelength of 532 nm was
410 employed to (1) selectively excite RB (note, EBS does not absorb light at 532 nm, see Figure S1
411 in the SI) and (2) avoid generation of other RB reactive intermediates (note, Allen *et al.* [46]
412 reported generation of RB radicals at 313 nm but not above 514 nm). The experimental data
413 confirmed that EBS reacts with $^3RB^{2-*}$. RB triplets can sensitize chemical degradation by energy
414 transfer (E_T = 171-176 kJ mol^{-1}) [23, 47] and/or electron transfer (reduction potential,
415 $E°*(^3RB*/RB^{-\bullet}) = 1.23\ V_{SHE}$) [47]. Schöneich *et al.* [48] reported the oxidation potential of EBS to be
416 1.59 V, higher than the reduction potential of $^3RB^{2-*}$. Based on these findings, the electron
417 transfer reaction mechanism of EBS with $^3RB^{2-*}$ is unlikely, and the energy transfer mechanism
418 is proposed. The Stern-Volmer plot in Figure S6 of the SI was used to determine the second-
419 order rate constant of $^3RB^{2-*}$ with EBS (*i.e.*, 4.30 (± 0.15) × 10^8 $M^{-1}s^{-1}$). Importantly, solution pH
420 did not influence the reaction kinetics (see Table S2 of the SI for second-order rate constants for
421 EBS reaction with $^3RB^{2-*}$). Criado *et al.* [22] highlighted the important role of $^3RB^{2-*}$ in the
422 photochemical degradation of tryptophan and its derivatives, which exhibited second-order
423 reaction rate constants with $^3RB^{2-*}$ on the order of 10^7 $M^{-1}s^{-1}$. Another study reported second-
424 order rate constants of 10^7- 10^8 $M^{-1}s^{-1}$ for neonicotinoids with $^3RB^{2-*}$ [49].
425
426 The pH-independent photoreaction kinetics of EBS with $^3RB^{2-*}$ (Figure S6 in the SI) and $^1O_2$
427 (postulated from the lack of acid dissociation and the consistent $^1O_2$ steady-state concentrations
428 in Figure 2a) suggest another mechanism contributes to the observed rate constants for EBS
429 degradation at high pH. While mechanistic evaluation of this reaction was beyond the scope of
430 this study, one possible explanation for the pH-dependent photodegradation kinetics observed in
431 Table 1 and Figure 2 may involve $O_2^{\bullet-}$. Previous pharmacological studies have indicated that

EBS undergoes reduction by $O_2^{\bullet-}$ [50, 51]. Lee *et al.* [24] reported that $^3RB^{2-*}$ quenching by molecular oxygen yields 75% $^1O_2$ and 20% $O_2^{\bullet-}$. While $O_2^{\bullet-}$ can undergo self-dismutation to form H_2O_2 [52], the rate of reaction exponentially decreased from pH 4.8 to pH 11 [53]. The effective concentration of $O_2^{\bullet-}$, therefore, increases at higher pH, potentially explaining the faster EBS photodegradation kinetics in RB-sensitized solutions at high pH. This hypothesis is supported by results from Chen *et al.* [54], who reported that a one-electron transfer mechanism for acetaminophen with $O_2^{\bullet-}$ was 1.1× faster at pH 10.0 than at pH 8.0. Given the faster EBS photodegradation kinetics at higher pH, the contribution of H_2O_2 generated through $O_2^{\bullet-}$ self-dismutation to EBS degradation was negligible.

Overall, the reported data suggest that investigation of the environmental photochemistry of organoselenium chemicals requires careful consideration of the protocols used to identify transformation mechanisms and calculate rate constants. Due to the higher reactivity of EBS with $^3RB^{2-*}$ (4.30 (± 0.15) × 10^8 $M^{-1}s^{-1}$) than $^1O_2$ (4.16 × 10^6 M^{-1} s^{-1} [9]), the common strategy of using RB-sensitized solutions to directly calculate $^1O_2$ reaction kinetics would result in overestimation of the second-order rate constant for EBS with $^1O_2$ and underestimation of the EBS half-life in the natural environment. Findings from this study emphasize the importance of $^3RB^{2-*}$, $^1O_2$, $O_2^{\bullet-}$, H_2O_2, and solution pH to the reaction mechanisms and kinetics of EBS, and presumably other organoselenium chemicals, in RB- and PN-sensitized solutions.

3.2.2 EBS reacts with $^{\bullet}$OH sensitizers

Previous antioxidant studies have determined that EBS is an excellent scavenger of H_2O_2, $OONO^-$, and other nitrite radicals [10, 34, 35]. As a result, conventional methods to generate $^{\bullet}OH$, including UV-H_2O_2, photo-Fenton, and solar irradiation of NO_3^- or NO_2^-, may complicate the evaluation of EBS kinetics due to secondary reactions with H_2O_2 and $OONO^-$. These methods of sensitizing $^{\bullet}OH$ cannot, therefore, be applied to determine the second-order rate constant for EBS reaction with $^{\bullet}OH$ without a means to prevent EBS reaction with H_2O_2 or $OONO^-$. While ascorbic acid [55], dehydroascorbic acid [55], thiosulfate [56], horseradish peroxidase [57, 58], and sodium pyruvate [59] have been used to quench H_2O_2, some of these chemicals generate intermediate radicals that may react with EBS [55, 56]. The reaction between sodium pyruvate and H_2O_2, however, yields non-radical products (see Eq. 9) and was, therefore, used to deconvolute the reaction kinetics of EBS with H_2O_2 and $^{\bullet}OH$.

$$CH_3COCOOH + H_2O_2 \rightarrow CH_3COOH + H_2O + CO_2 \qquad \text{(Eq. 9)}$$

Dark experiments were conducted with EBS and H_2O_2 at pH 7.1. Upon collection, the samples were immediately mixed with 7.5 mM sodium pyruvate to quench the reaction; note, Figure S7 of the SI demonstrates that sodium pyruvate was an efficient quencher of residual H_2O_2. The pseudo-first-order reaction kinetics expression in Eq. 1 was applied to calculate k''_{EBS,H_2O_2}, which was determined to be 79.8 ± 0.8 M^{-1} s^{-1}. Using the calculated $k''_{EBS,H_2O_2}$and the second-order rate constant for sodium pyruvate quenching of H_2O_2 (*i.e.*, 0.75 M^{-1} s^{-1} [60]), the quenching reaction was verified to be 95% efficient. Two different k''_{EBS,H_2O_2} values have been reported in the literature: 1100 M^{-1} s^{-1} [61]; and, 4.83 M^{-1} s^{-1} [62]. The inconsistency in previously reported values

might stem from interference by EBS transformation products during spectrophotometric analysis of EBS. In those studies, the normalized absorbance at 330 nm was linearly correlated to the normalized EBS concentration, and the second-order rate constant for EBS was calculated according to Eq. 1. Under the tested conditions, the reaction between EBS and H_2O_2 forms ebselen selenoxide [63], which interferes with spectrophotometric analyses (Figure S1 of the SI). This interference was not observed during the LC-MS/MS analysis used in the present study (see Figure S8 of SI), providing higher confidence in the reported second-order rate constant.

Competition kinetics experiments with *p*CBA were conducted to calculate the second-order rate constants for •OH reaction with EBS and C-EBS. The observed degradation trends for direct photolysis at 254 nm, UV-H_2O_2 treatment, and (dark) reaction with H_2O_2 are shown in Figure 3 (EBS and C-EBS) and Figure S9 in the SI (*p*CBA). In Figure 3, the reaction between EBS and H_2O_2 is negligible in the dark due to pyruvate quenching of residual H_2O_2. The second-order rate constants for EBS and C-EBS with •OH were calculated to be 4.33 (± 0.26) × 10^{10} M^{-1} s^{-1} and 1.76 (± 0.32) × 10^{8} M^{-1} s^{-1}, respectively, at pH 7.1. The high rate constant of EBS with •OH reinforces the reactivity of EBS with reactive oxygen species. The selenium atom enhanced the chemical reactivity by two orders of magnitude. Although k''_{EBS,H_2O_2} (*i.e.*, 79.8 ± 0.8 M^{-1} s^{-1}) is orders of magnitude lower than the rate constants for EBS reaction with $^1O_2$, •OH, and other reactive species, the H_2O_2 concentration was much higher. Therefore, the reaction of EBS with H_2O_2 during sample preparation (prior to irradiation) and after sample collection (during storage) can lead to inaccurate rate constants if a suitable H_2O_2 scavenger is not used.

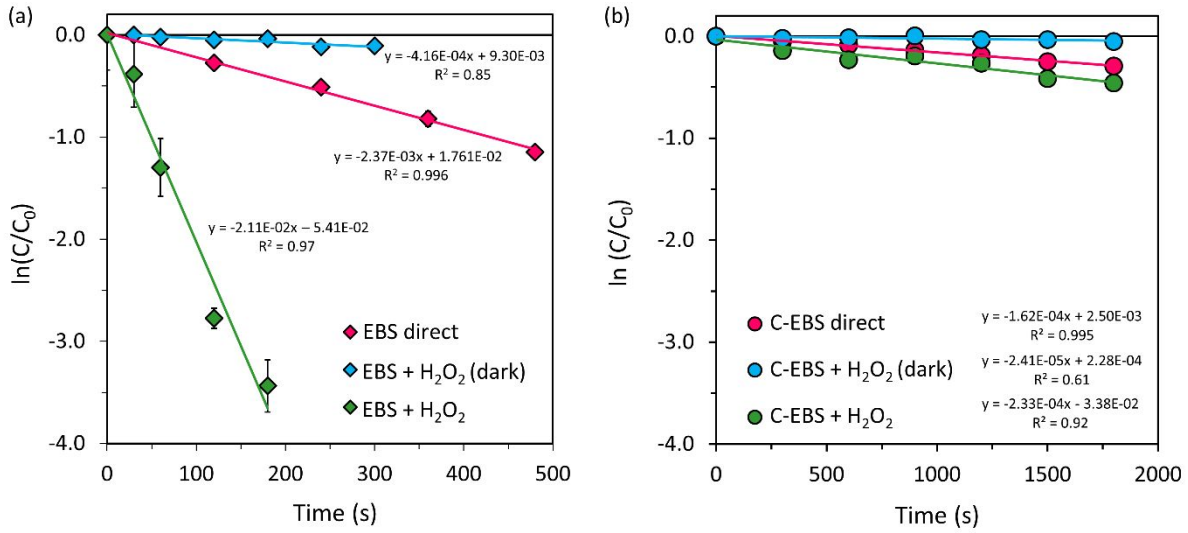

Figure 3. Degradation of 3.6 µM (a) EBS and (b) C-EBS at pH 7.1 for direct photolysis at 254 nm, UV-H_2O_2 treatment (254 nm), and reaction with H_2O_2 in the dark. The initial H_2O_2 concentrations were 5 µM for EBS and 5 mM for C-EBS to generate higher steady-state •OH concentrations. Due to its high reactivity with EBS, residual H_2O_2 was quenched by 7.5 mM sodium pyruvate for solutions in (a). The plotted symbols represent the mean of triplicate experiments, and the error bars are standard deviation.

3.3 Interaction of EBS with reactive species quenchers

The effects of select reactive species quenchers and scavengers on EBS photodegradation were evaluated. Since C-EBS is not a contaminant of interest, the confounding effects of reactive species quenchers and scavengers were not investigated. Figure 4a shows that when 0.5 mM sorbic acid was added to investigate the self-sensitized degradation of EBS at 365 nm and pH 6.8, the measured rate constant (*i.e.*, 2.36 (± 0.49) × 10^{-4} s^{-1}) was greater than the direct photolysis rate constant for EBS (*i.e.*, 4.86 (± 1.00) × 10^{-5} s^{-1}). With addition of sorbic acid, the

observed rate constants for EBS degradation were expected to be similar (if no self-sensitization) or lower (if self-sensitization). The unexpected enhancement in EBS degradation kinetics can be explained by energy quenching from excited sorbic acid. Grebel *et al.* [64] indicated that sorbic acid can undergo direct photoisomerization at high concentrations due to a small overlap in the sorbic acid absorbance spectrum (which extended beyond 310 nm) and the emission spectrum of lamps. Here, the lamp spectrum spanned 310-410 nm, and 0.5 mM sorbic acid was used. According to Grebel *et al.* [64], these conditions are expected to generate triplets in the experimental solutions. Moor *et al.* [28] reported the triplet excited energy of sorbic acid to be in the 187-217 kJ mol^{-1} range. As indicated in section 3.2.1, EBS undergoes an energy transfer mechanism with $^3RB^{2-}$*, which has a triplet excited energy of 171-176 kJ mol^{-1} [23, 47]; therefore, a similar energy transfer reaction mechanism is expected to occur with sorbic acid triplets.

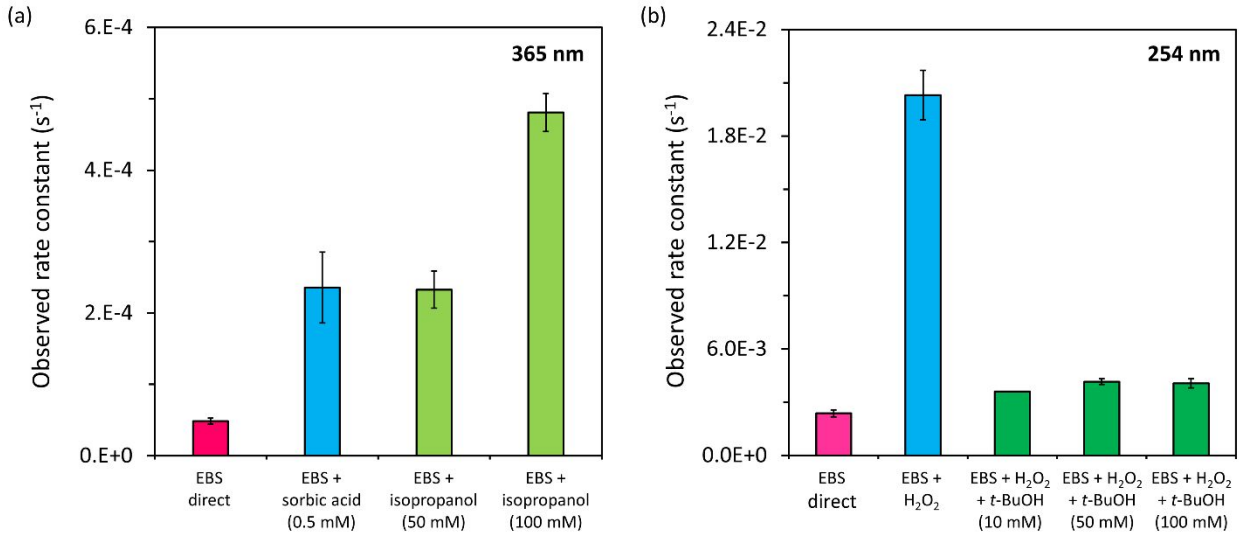

Figure 4. Comparison of observed rate constants for EBS degradation at (a) 365 nm with 0.5 mM sorbic acid and 50-100 mM isopropanol and (b) 254 nm with 5 µM H_2O_2 and 0, 10, 50, and 100 mM tert-butanol. The solution pH was 6.8. Error bars represent 95% confidence intervals on the mean rate constant from triplicate time series experiments (n = 7 × 3 = 21).

As suggested by Figure 4a, EBS reacted with isopropanol and active intermediates of isopropanol that was produced during irradiation. The rate constant for EBS degradation was dependent on the isopropanol concentration, with calculated values of 2.33 (± 0.26) × 10^{-4} s^{-1} and 4.81 (± 0.27) × 10^{-4} s^{-1} for 50 mM and 100 mM isopropanol, respectively. The observed rate constants were one order of magnitude faster than direct photolysis of EBS at 365 nm (*i.e.*, 4.86 (± 1.00) × 10^{-5} s^{-1}). EBS also reacted with isopropanol in the dark, and the second-order rate constant was calculated to be 4.6 (± 1.2) × 10^{-4} $M^{-1}s^{-1}$. Packer *et al.* [29] reported similar observations with diclofenac and clofibric acid, namely isopropanol increased the photodegradation rate. Enhanced degradation of diclofenac and clofibric acid was attributed to active intermediates of isopropanol and photoreduction mechanisms [29]. If $EBS^{\bullet+}$ is formed upon irradiation, hydrogen atom transfer from isopropanol might lead to secondary reactions between hydroxyisopropyl radicals and EBS [65].

Figure S10 in the SI reports EBS degradation with 0, 1, and 10 mM NaN_3 at pH 4, 6, 8, and 10. These experiments were primarily designed to investigate the potential involvement of self-sensitized degradation of EBS at 254 nm and 365 nm with respect to the pH dependencies observed in section 3.1. At 365 nm, the addition of NaN_3 demonstrated no effect on EBS degradation. However, convoluted effects, similar to those reported for sorbic acid and isopropanol, were observed with NaN_3 at 254 nm. In particular, EBS exhibited enhanced degradation in the presence of NaN_3, and not the similar (if no self-sensitization) or lower (if self-sensitization) reaction rates that were expected. At pH 4, the addition of 1 mM and 10 mM

556 NaN_3 increased photodegradation rates of EBS by 1.4× and 2.5×, respectively, compared to the 0
557 mM NaN_3 condition (see Figure S10 in the SI). At pH 10, the observed rate constants for EBS
558 degradation in solutions containing 0, 1, and 10 mM NaN_3 were 2.9×, 6.0×, and 20.1× faster,
559 respectively, than for pH 4 solutions with 0 mM NaN_3. Note that the apparent molar absorption
560 coefficient of NaN_3 at 254 nm was 84.6 M^{-1} cm^{-1}, and screening corrections were applied to the
561 measured rate constants. Previous studies have reported azide radical (strong oxidant) formation
562 through azide anion reaction with reactive oxygen species (*e.g.*, $^1O_2$, $O_2^{\bullet-}$, $^{\bullet}OH$) [45, 66, 67],
563 potentially explaining the faster EBS rate constants observed at higher NaN_3 concentrations.
564 Future investigations are necessary to further deconvolute the observed reaction kinetics of EBS
565 with NaN_3, but these efforts were outside of the scope of this study. The reported findings
566 suggest that NaN_3 should be avoided when studying EBS degradation kinetics; note, these results
567 are also relevant to biological systems where NaN_3 is often used to inactivate microbial growth
568 [67, 68].
569
570 In the absence of H_2O_2, interactions between EBS and *tert*-butanol were not observed during
571 irradiation experiments with 0 and 50 mM *tert*-butanol (p = 0.71, ANCOVA). In the UV-H_2O_2
572 process, however, enhanced degradation of EBS was observed when *tert*-butanol was used as a
573 $^{\bullet}OH$ quencher. Schewe [5] and Kamigata *et al.* [69] suggested that the secondary organic radicals
574 (*e.g.*, $R^{\bullet}$ and $ROO^{\bullet}$) formed by *tert*-butanol reaction with $^{\bullet}OH$ would react with EBS. From
575 Figure 4b, the observed rate constants for direct photolysis of EBS at 254 nm, UV-H_2O_2
576 treatment of EBS, and UV-H_2O_2 treatment of EBS in the presence of *tert*-butanol were 2.37 (±
577 0.20) × 10^{-3} s^{-1}, 2.03 (± 0.13) × 10^{-2} s^{-1}, and 4.16 (± 0.16) × 10^{-3} s^{-1}, respectively. Three
578 concentrations of *tert*-butanol, namely 10, 50, and 100 mM, were used to ensure that the

enhanced degradation was not from residual $^{\bullet}OH$. In all three cases, the observed rate constants were similar (see Figure 4b), suggesting efficient quenching of $^{\bullet}OH$ by *tert*-butanol and confirming EBS reaction with secondary organic radicals.

The reported data highlight the complex photochemistry of organoselenium compounds, which are being increasingly used for pharmaceutical applications and represent unique contaminants of emerging concern. More studies on EBS occurrence in water resources and fate in biological and photochemical processes are needed to determine EBS persistence, and potential toxicity outcomes, in the environment. The fast phototransformation kinetics reported here suggest EBS does not persist in engineered or natural systems. However, conventional protocols would have overestimated EBS degradation because the chemicals used for sensitizing and quenching reactive species exhibited convoluted effects on EBS photodegradation due to generation of kinetically-relevant active intermediates (*i.e.*, isopropanol, NaN_3, PN, RB, sorbic acid, *tert*-butanol) or direct reaction with EBS (*i.e.*, H_2O_2, isopropanol). These complications stem from the antioxidant properties of organoselenium chemicals. RB- and PN-sensitized reactions were partially quenched with NaN_3, but the quenching efficiency was lower at higher pH for both $^1O_2$ sensitizers, potentially due to EBS reduction by $O_2^{\bullet-}$. The high reactivity of EBS with active intermediates will also affect the assessment of EBS degradation during photocatalysis [70], ozonation [70], and other processes involving reactive species. Overall, the complex reactions of EBS with commonly employed reactive species sensitizers, scavengers, and quenchers presented in this study will provide insight into future research of organoselenium chemicals in the environment. For the same reasons, EBS may serve as an advantageous quenching agent that can be adopted for a variety of reactive oxygen species.

602

603

604 **SUPPORTING INFORMATION**

605

606 Chemicals; analytical methods; quantum yield calculations; transient adsorption spectroscopy;
607 triplets and active intermediates formed by reactive species sensitizers and quenchers; EBS rate
608 constants with $^3RB^{2-*}$; molar adsorption coefficients; effect of phosphate buffer on EBS
609 degradation; $^1O_2$ rate constants from PN-photosensitized system; C-EBS degradation kinetics in
610 RB-photosensitized system; Stern-Volmer plot for $^3RB^{2-*}$ decay with EBS; efficacy of pyruvate
611 H_2O_2 quencher; formation of ebselen selenoxide; *p*CBA degradation kinetics; and, EBS
612 photodegradation in presence of NaN_3.

613

614

615 **ACKNOWLEDGEMENT**

616

617 We acknowledge funding from the National Science Foundation (CHE 1508090).

REFERENCES

1. Zhang, M.; Nomura, A.; Uchida, Y.; Iijima, H.; Sakamoto, T.; Iishii, Y.; Morishima, Y.; Mochizuki, M.; Masuyama, K.; Hirano, K.; Sekizawa, K., Ebselen suppresses late airway responses and airway inflammation in guinea pigs. *Free Radical Biology and Medicine* **2002,** *32*, (5), 454-64.
2. Sarma, B. K.; Mugesh, G., Antioxidant activity of the anti-inflammatory compound ebselen: a reversible cyclization pathway via selenenic and seleninic acid intermediates. *Chemistry (Weinheim an der Bergstrasse, Germany)* **2008,** *14*, (34), 10603-14.
3. Prasad, N.; Ramteke, P.; Dholia, N.; Yadav, U. C. S., Chapter 27 - Therapeutic interventions to block oxidative stress-associated pathologies. In *Immunity and Inflammation in Health and Disease*, Chatterjee, S.; Jungraithmayr, W.; Bagchi, D., Eds. Academic Press: 2018; pp 341-362.
4. Bartolini, D.; Sancineto, L.; Fabro de Bem, A.; Tew, K. D.; Santi, C.; Radi, R.; Toquato, P.; Galli, F., Chapter Ten - Selenocompounds in cancer therapy: An overview. In *Advances in Cancer Research*, Tew, K. D.; Galli, F., Eds. Academic Press: 2017; Vol. 136, pp 259-302.
5. Schewe, T., Molecular actions of Ebselen—an antiinflammatory antioxidant. *General Pharmacology: The Vascular System* **1995,** *26*, (6), 1153-1169.
6. Thangamani, S.; Younis, W.; Seleem, M. N., Repurposing ebselen for treatment of multidrug-resistant staphylococcal infections. *Scientific Reports* **2015,** *5*, 11596.
7. Gustafsson, T. N.; Osman, H.; Werngren, J.; Hoffner, S.; Engman, L.; Holmgren, A., Ebselen and analogs as inhibitors of Bacillus anthracis thioredoxin reductase and bactericidal antibacterials targeting Bacillus species, Staphylococcus aureus and Mycobacterium

tuberculosis. *Biochimica et Biophysica Acta (BBA)-General Subjects* **2016,** *1860*, (6), 1265-1271.

8. Jin, Z.; Du, X.; Xu, Y.; Deng, Y.; Liu, M.; Zhao, Y.; Zhang, B.; Li, X.; Zhang, L.; Peng, C.; Duan, Y.; Yu, J.; Wang, L.; Yang, K.; Liu, F.; Jiang, R.; Yang, X.; You, T.; Liu, X.; Yang, X.; Bai, F.; Liu, H.; Liu, X.; Guddat, L. W.; Xu, W.; Xiao, G.; Qin, C.; Shi, Z.; Jiang, H.; Rao, Z.; Yang, H., Structure of Mpro from SARS-CoV-2 and discovery of its inhibitors. *Nature* **2020,** *582*, (7811), 289-293.
9. Mishra, B.; Priyadarsini, K. I.; Mohan, H.; Mugesh, G., Horseradish peroxidase inhibition and antioxidant activity of ebselen and related organoselenium compounds. *Bioorganic & Medicinal Chemistry Letters* **2006,** *16*, (20), 5334-5338.
10. Masumoto, H.; Kissner, R.; Koppenol, W. H.; Sies, H., Kinetic study of the reaction of ebselen with peroxynitrite. *Federation of European Biochemical Societies Letters* **1996,** *398*, (2-3), 179-82.
11. Azad, G. K.; Tomar, R. S., Ebselen, a promising antioxidant drug: mechanisms of action and targets of biological pathways. *Molecular Biology Reports* **2014,** *41*, (8), 4865-4879.
12. Azad, G. K.; Balkrishna, S. J.; Sathish, N.; Kumar, S.; Tomar, R. S., Multifunctional ebselen drug functions through the activation of DNA damage response and alterations in nuclear proteins. *Biochemical Pharmacology* **2012,** *83*, (2), 296-303.
13. Miorelli, S. T.; Rosa, R. M.; Moura, D. J.; Rocha, J. C.; Carneiro Lobo, L. A.; Pêgas Henriques, J. A.; Saffi, J., Antioxidant and anti-mutagenic effects of ebselen in yeast and in cultured mammalian V79 cells. *Mutagenesis* **2008,** *23*, (2), 93-99.

14. Simmons, D. B. D.; Wallschla ger, D., A critical review of the biogeochemistry and ecotoxicology of selenium in lotic and lentic environments. *Environmental Toxicology and Chemistry* **2005,** *24 6*, 1331-43.

15. Lemly, A. D., Aquatic selenium pollution is a global environmental safety issue. *Ecotoxicology and Environmental Safety* **2004,** *59*, (1), 44-56.

16. EPA, Aquatic life ambient water quality criterion for selenium in freshwater. Available at www.epa.gov/wqc/aquatic-life-criterion-selenium. Accessed on August 8, 2020.

17. Hopanna, M.; Mangalgiri, K.; Ibitoye, T.; Ocasio, D.; Snowberger, S.; Blaney, L., Chapter 8 - UV-254 transformation of antibiotics in water and wastewater treatment processes. In *Contaminants of Emerging Concern in Water and Wastewater*, Hernández-Maldonado, A. J.; Blaney, L., Eds. Butterworth-Heinemann: 2020; pp 239-297.

18. Adak, A.; Mangalgiri, K. P.; Lee, J.; Blaney, L., UV irradiation and UV-H2O2 advanced oxidation of the roxarsone and nitarsone organoarsenicals. *Water Research* **2015,** *70*, 74-85.

19. Chu, C.; Stamatelatos, D.; McNeill, K., Aquatic indirect photochemical transformations of natural peptidic thiols: impact of thiol properties, solution pH, solution salinity and metal ions. *Environmental Science: Processes & Impacts* **2017,** *19*, (12), 1518-1527.

20. Remucal, C. K., The role of indirect photochemical degradation in the environmental fate of pesticides: a review. *Environmental Science: Processes & Impacts* **2014,** *16*, (4), 628-653.

21. McConville, M. B.; Mezyk, S. P.; Remucal, C. K., Indirect photodegradation of the lampricides TFM and niclosamide. *Environmental Science: Processes & Impacts* **2017,** *19*, (8), 1028-1039.

22. Criado, S.; Bertolotti, S. G.; García, N. A., Kinetic aspects of the rose bengal-sensitized photo-oxygenation of tryptophan alkyl esters. Ground state and photopromoted dye-

684 tryptophan derivative interactions. *Journal of Photochemistry and Photobiology B: Biology*
685 **1996,** *34*, (1), 79-86.
686 23. Ludvikova, L.; Fris, P.; Heger, D.; Sebej, P.; Wirz, J.; Klan, P., Photochemistry of rose
687 bengal in water and acetonitrile: a comprehensive kinetic analysis. *Physical Chemistry*
688 *Chemical Physics : PCCP* **2016,** *18*, (24), 16266-73.
689 24. Lee, P. C.; Rodgers, M. A., Laser flash photokinetic studies of rose bengal sensitized
690 photodynamic interactions of nucleotides and DNA. *Photochemistry and Photobiology* **1987,**
691 *45*, (1), 79-86.
692 25. Stathis, A. A.; Hendrickson-Stives, A. K.; Kahan, T. F., Photolysis kinetics of toluene,
693 ethylbenzene, and xylenes at ice surfaces. *The Journal of Physical Chemistry A* **2016,** *120*,
694 (34), 6693-6697.
695 26. Davis, C. A.; Erickson, P. R.; McNeill, K.; Janssen, E. M. L., Environmental photochemistry
696 of fenamate NSAIDs and their radical intermediates. *Environmental Science: Processes &*
697 *Impacts* **2017,** *19*, (5), 656-665.
698 27. Neckers, D. C.; Jenks, W. S.; Wolff, T., *Advances in Photochemistry*. Wiley, 2007: Hoboken,
699 N.J., 2007; Vol. 29.
700 28. Moor, K. J.; Schmitt, M.; Erickson, P. R.; McNeill, K., Sorbic acid as a triplet probe: Triplet
701 energy and reactivity with triplet-state dissolved organic matter via $^1O_2$ phosphorescence.
702 *Environmental Science & Technology* **2019,** *53*, (14), 8078-8086.
703 29. Packer, J. L.; Werner, J. J.; Latch, D. E.; McNeill, K.; Arnold, W. A., Photochemical fate of
704 pharmaceuticals in the environment: Naproxen, diclofenac, clofibric acid, and ibuprofen.
705 *Aquatic Sciences* **2003,** *65*, (4), 342-351.

706 30. Mangalgiri, K. P.; Blaney, L., Elucidating the stimulatory and inhibitory effects of dissolved
707 organic matter from poultry litter on photodegradation of antibiotics. *Environmental Science*
708 *& Technology* **2017,** *51*, (21), 12310-12320.
709 31. Bolton, J. R.; Stefan, M. I.; Shaw, P.-S.; Lykke, K. R., Determination of the quantum yields
710 of the potassium ferrioxalate and potassium iodide–iodate actinometers and a method for the
711 calibration of radiometer detectors. *Journal of Photochemistry and Photobiology A:*
712 *Chemistry* **2011,** *222*, (1), 166-169.
713 32. Appiani, E.; Ossola, R.; Latch, D. E.; Erickson, P. R.; McNeill, K., Aqueous singlet oxygen
714 reaction kinetics of furfuryl alcohol: effect of temperature, pH, and salt content.
715 *Environmental Science: Processes & Impacts* **2017,** *19*, (4), 507-516.
716 33. Gligorovski, S.; Strekowski, R.; Barbati, S.; Vione, D., Environmental implications of
717 hydroxyl radicals (• OH). *Chemical Reviews* **2015,** *115*, (24), 13051-13092.
718 34. Masumoto, H.; Sies, H., The reaction of ebselen with peroxynitrite. *Chemical Research in*
719 *Toxicology* **1996,** *9*, (1), 262-7.
720 35. Haenen, G. R.; De Rooij, B. M.; Vermeulen, N. P.; Bast, A., Mechanism of the reaction of
721 ebselen with endogenous thiols: dihydrolipoate is a better cofactor than glutathione in the
722 peroxidase activity of ebselen. *Molecular Pharmacology* **1990,** *37*, (3), 412-22.
723 36. Pi, Y.; Schumacher, J.; Jekel, M., Decomposition of aqueous ozone in the presence of
724 aromatic organic solutes. *Water Research* **2005,** *39*, (1), 83-88.
725 37. Pi, Y.; Schumacher, J.; Jekel, M., The use of *para*-chlorobenzoic acid (*p*CBA) as an
726 ozone/hydroxyl radical probe compound. *Ozone: Science & Engineering* **2005,** *27*, (6), 431-
727 436.
728 38. ChemAxon https://chemicalize.com/ (February 20, 2018),

729 39. Sheraz, M. A.; Kazi, S. H.; Ahmed, S.; Mirza, T.; Ahmad, I.; Evstigneev, M. P., Effect of
730 phosphate buffer on the complexation and photochemical interaction of riboflavin and
731 caffeine in aqueous solution: A kinetic study. *Journal of Photochemistry and Photobiology*
732 *A: Chemistry* **2014,** *273*, 17-22.
733 40. Ahmad, I.; Fasihullah, Q.; Vaid, F. H. M., Effect of phosphate buffer on photodegradation
734 reactions of riboflavin in aqueous solution. *Journal of Photochemistry and Photobiology B:*
735 *Biology* **2005,** *78*, (3), 229-234.
736 41. Di Mascio, P.; Martinez, G. R.; Miyamoto, S.; Ronsein, G. E.; Medeiros, M. H. G.; Cadet, J.,
737 Singlet molecular oxygen reactions with nucleic acids, lipids, and proteins. *Chemical*
738 *Reviews* **2019,** *119*, (3), 2043-2086.
739 42. Rogers, J. E.; Kelly, L. A., Nucleic acid oxidation mediated by naphthalene and
740 benzophenone imide and diimide derivatives: consequences for DNA redox chemistry.
741 *Journal of the American Chemical Society* **1999,** *121*, (16), 3854-3861.
742 43. Abraham, B.; McMasters, S.; Mullan, M. A.; Kelly, L. A., Reactivities of carboxyalkyl-
743 substituted 1,4,5,8-naphthalene diimides in aqueous solution. *Journal of the American*
744 *Chemical Society* **2004,** *126*, (13), 4293-4300.
745 44. Apell, J. N.; Pflug, N. C.; McNeill, K., Photodegradation of fludioxonil and other pyrroles:
746 the importance of indirect photodegradation for understanding environmental fate and
747 photoproduct formation. *Environmental Science & Technology* **2019,** *53*, (19), 11240-11250.
748 45. Harbour, J. R.; Issler, S. L., Involvement of the azide radical in the quenching of singlet
749 oxygen by azide anion in water. *Journal of the American Chemical Society* **1982,** *104*, (3),
750 903-905.

751 46. Allen, M. T.; Lynch, M.; Lagos, A.; Redmond, R. W.; Kochevar, I. E., A wavelength
752 dependent mechanism for rose bengal-sensitized photoinhibition of red cell
753 acetylcholinesterase. *Biochimica et Biophysica Acta (BBA) - General Subjects* **1991,** *1075*,
754 (1), 42-49.
755 47. McNeill, K.; Canonica, S., Triplet state dissolved organic matter in aquatic photochemistry:
756 reaction mechanisms, substrate scope, and photophysical properties. *Environmental Science:*
757 *Processes & Impacts* **2016,** *18*, (11), 1381-1399.
758 48. Schöneich, C.; Narayanaswami, V.; Asmus, K.-D.; Sies, H., Reactivity of ebselen and related
759 selenoorganic compounds with 1, 2-dichloroethane radical cations and halogenated peroxyl
760 radicals. *Archives of Biochemistry and Biophysics* **1990,** *282*, (1), 18-25.
761 49. Dell'Arciprete, M. L.; Santos-Juanes, L.; Arques, A.; Vercher, R. F.; Amat, A. M.; Furlong,
762 J. P.; Mártire, D. O.; Gonzalez, M. C., Reactivity of neonicotinoid pesticides with singlet
763 oxygen. *Catalysis Today* **2010,** *151*, (1), 137-142.
764 50. Wang, J. F.; Komarov, P.; Sies, H.; de Groot, H., Inhibition of superoxide and nitric oxide
765 release and protection from reoxygenation injury by Ebselen in rat Kupffer cells. *Hepatology*
766 **1992,** *15*, (6), 1112-1116.
767 51. Araki, T.; Kitaoka, H., The mechanism of reaction of ebselen with superoxide in aprotic
768 solvents as examined by cyclic voltammetry and ESR. *Chemical and Pharmaceutical*
769 *Bulletin* **2001,** *49*, (5), 541-545.
770 52. Van Hemmen, J. J.; Meuling, W. J. A., Inactivation of biologically active DNA by γ-ray-
771 induced superoxide radicals and their dismutation products singlet molecular oxygen and
772 hydrogen peroxide. *Biochimica et Biophysica Acta (BBA) - Nucleic Acids and Protein*
773 *Synthesis* **1975,** *402*, (2), 133-141.

53. Samuel, E. L. G.; Marcano, D. C.; Berka, V.; Bitner, B. R.; Wu, G.; Potter, A.; Fabian, R. H.; Pautler, R. G.; Kent, T. A.; Tsai, A.-L.; Tour, J. M., Highly efficient conversion of superoxide to oxygen using hydrophilic carbon clusters. *Proceedings of the National Academy of Sciences of the United States of America* **2015,** *112*, (8), 2343-2348.

54. Chen, Y.; Zhang, X.; Feng, S., Contribution of the excited triplet state of humic acid and superoxide radical anion to generation and elimination of phenoxyl radical. *Environmental Science & Technology* **2018,** *52*, (15), 8283-8291.

55. Kamrul, H. S. M.; Schiraldi, A.; Cosio, M. S.; Scampicchio, M., Food and ascorbic scavengers of hydrogen peroxide. *Journal of Thermal Analysis and Calorimetry* **2016,** *125*, (2), 729-737.

56. Rochelle, G. T.; Owens, D. R.; Chang, J. C. S.; Bma, T. G., Thiosulfate as an oxidation inhibitor in flue gas desulfurization processes: a review of R&D results. *Journal of the Air Pollution Control Association* **1986,** *36*, (10), 1138-1146.

57. Miura, T.; Muraoka, S.; Fujimoto, Y., Lipid peroxidation induced by indomethacin with horseradish peroxidase and hydrogen peroxide: involvement of indomethacin radicals. *Biochemical Pharmacology* **2002,** *63*, (11), 2069-2074.

58. Rodríguez-López, J. N.; Lowe, D. J.; Hernández-Ruiz, J.; Hiner, A. N. P.; García-Cánovas, F.; Thorneley, R. N. F., Mechanism of reaction of hydrogen peroxide with horseradish peroxidase: identification of intermediates in the catalytic cycle. *Journal of the American Chemical Society* **2001,** *123*, (48), 11838-11847.

59. Long, L. H.; Halliwell, B., Artefacts in cell culture: Pyruvate as a scavenger of hydrogen peroxide generated by ascorbate or epigallocatechin gallate in cell culture media. *Biochemical and Biophysical Research Communications* **2009,** *388*, (4), 700-704.

797 60. Schöne, L.; Herrmann, H., Kinetic measurements on the reactivity of hydrogen peroxide and
798 ozone towards small atmospherically relevant aldehydes, ketones and organic acids in
799 aqueous solution. *Atmospheric Chemistry & Physics Discussions* **2013,** *13*, 25537-25566.
800 61. Maiorino, M.; Roveri, A.; Coassin, M.; Ursini, F., Kinetic mechanism and substrate
801 specificity of glutathione peroxidase activity of ebselen (PZ51). *Biochemical Pharmacology*
802 **1988,** *37*, (11), 2267-71.
803 62. Morgenstern, R.; Cotgreave, I. A.; Engman, L., Determination of the relative contributions of
804 the diselenide and selenol forms of ebselen in the mechanism of its glutathione peroxidase-
805 like activity. *Chemico-Biological Interactions* **1992,** *84*, (1), 77-84.
806 63. Sies, H., Ebselen, a selenoorganic compound as glutathione peroxidase mimic. *Free Radical*
807 *Biology and Medicine* **1993,** *14*, (3), 313-323.
808 64. Grebel, J. E.; Pignatello, J. J.; Mitch, W. A., Sorbic acid as a quantitative probe for the
809 formation, scavenging and steady-state concentrations of the triplet-excited state of organic
810 compounds. *Water Research* **2011,** *45*, (19), 6535-6544.
811 65. Schwack, W.; Bourgeois, B.; Walker, F., Fungicides and photochemistry photodegradation
812 of the dicarboximide fungicide procymidone. *Chemosphere* **1995,** *31*, (9), 4033-4040.
813 66. Roberts, J. E.; Wishart, J. F.; Martinez, L.; Chignell, C. F., Photochemical studies on
814 xanthurenic acid. *Photochemistry and Photobiology* **2000,** *72*, (4), 467-471.
815 67. Huang, L.; St Denis, T. G.; Xuan, Y.; Huang, Y.-Y.; Tanaka, M.; Zadlo, A.; Sarna, T.;
816 Hamblin, M. R., Paradoxical potentiation of methylene blue-mediated antimicrobial
817 photodynamic inactivation by sodium azide: role of ambient oxygen and azide radicals. *Free*
818 *Radical Biology & Medicine* **2012,** *53*, (11), 2062-2071.

819 68. Kasimova, K. R.; Sadasivam, M.; Landi, G.; Sarna, T.; Hamblin, M. R., Potentiation of
820 photoinactivation of Gram-positive and Gram-negative bacteria mediated by six
821 phenothiazinium dyes by addition of azide ion. *Photochemical and Photobiological Sciences*
822 **2014,** *13*, (11), 1541-8.
823 69. Nobumasa, K.; Hirokazu, I.; Akira, I.; Michio, K., Photochemical reaction of 2-Aryl-1,2-
824 benzisoselenazol-3(2H)-ones. *Bulletin of the Chemical Society of Japan* **1986,** *59*, (7), 2179-
825 2183.
826 70. Chen, S.; Blaney, L.; Chen, P.; Deng, S.; Hopanna, M.; Bao, Y.; Yu, G., Ozonation of the 5-
827 fluorouracil anticancer drug and its prodrug capecitabine: Reaction kinetics, oxidation
828 mechanisms, and residual toxicity. *Frontiers of Environmental Science & Engineering* **2019,**
829 *13*, (4), 59.
830